

Sulfur-doped porous reduced graphene oxide hollow nanospheres framework as metal-free electrocatalysts for oxygen reduction reaction and supercapacitor electrode materials

Xi'an Chen^{a,b}, Xiaohua Chen^{a,*}, Xin Xu^b, Zhi Yang^b, Zheng Liu^a, Lijie, Zhang^b, Xiangju, Xu^b, Ying Chen^c and Shaoming Huang^{b,*}

^a College of Materials Science and Engineering, Hunan University, Hunan Province Key Laboratory for Spray Deposition Technology and Application, Changsha 410082, P. R. China. E-mail: hudacxh@qq.com.

^b Zhejiang Key Laboratory of Carbon Materials, College of Chemistry and materials engineering, Wenzhou University, Wenzhou 325027, P. R. China. E-mail: smhuang@wzu.edu.cn.

^c ARC Centre of Excellence for Functional Nanomaterials, Institute for Frontier Materials, Deakin University, Waurn Ponds, Victoria 3216, Australia.

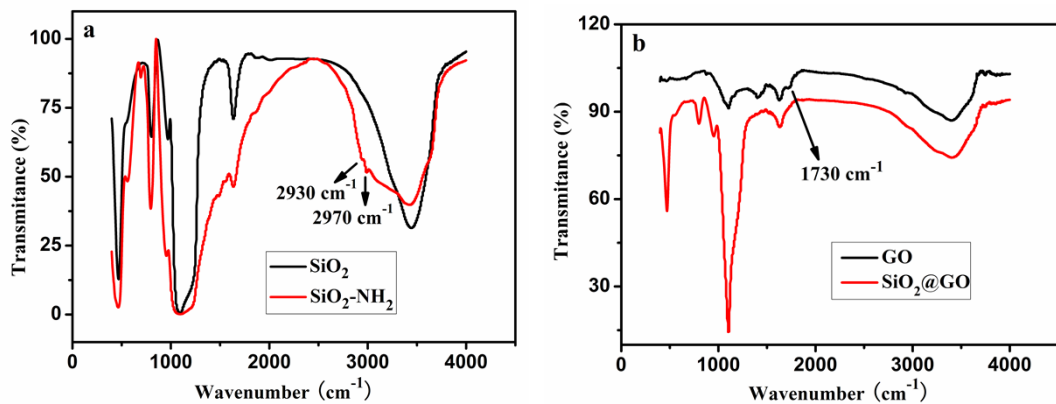


Fig. S1 FT-IR spectra of SiO_2 and $\text{SiO}_2\text{-NH}_2$ (a), GO and $\text{SiO}_2\text{@GO}$ (b).

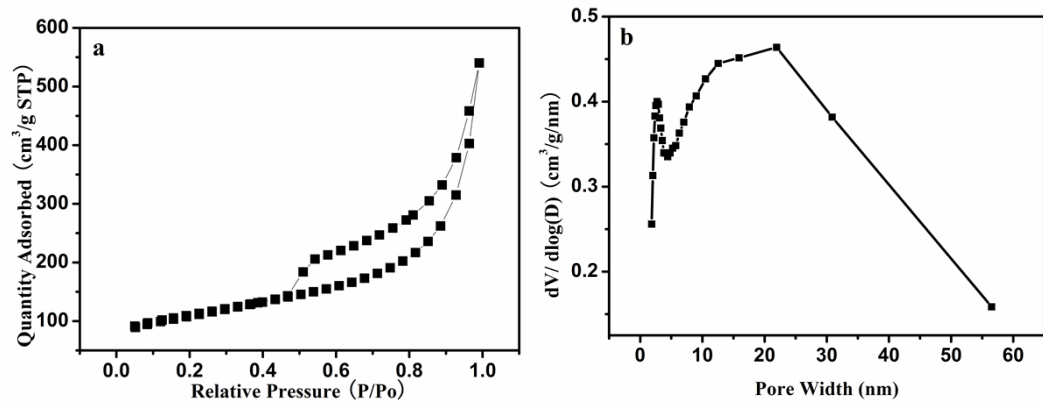


Fig. S2 (a) N_2 sorption isotherm; (b) pore size distribution of S-PGHS-900 sample.

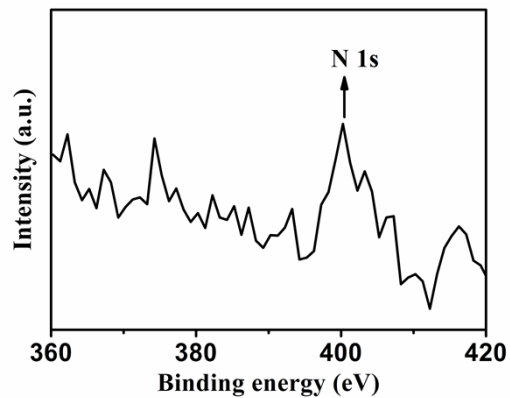


Fig. S3 XPS N1s spectrum of S-PGHS-900

Table S1 Elemental analysis of the S-PGHS-900

| elements | C | H | S | N |
|----------|-------|-------|-------|------|
| content | 80.65 | 2.082 | 3.028 | 0.14 |

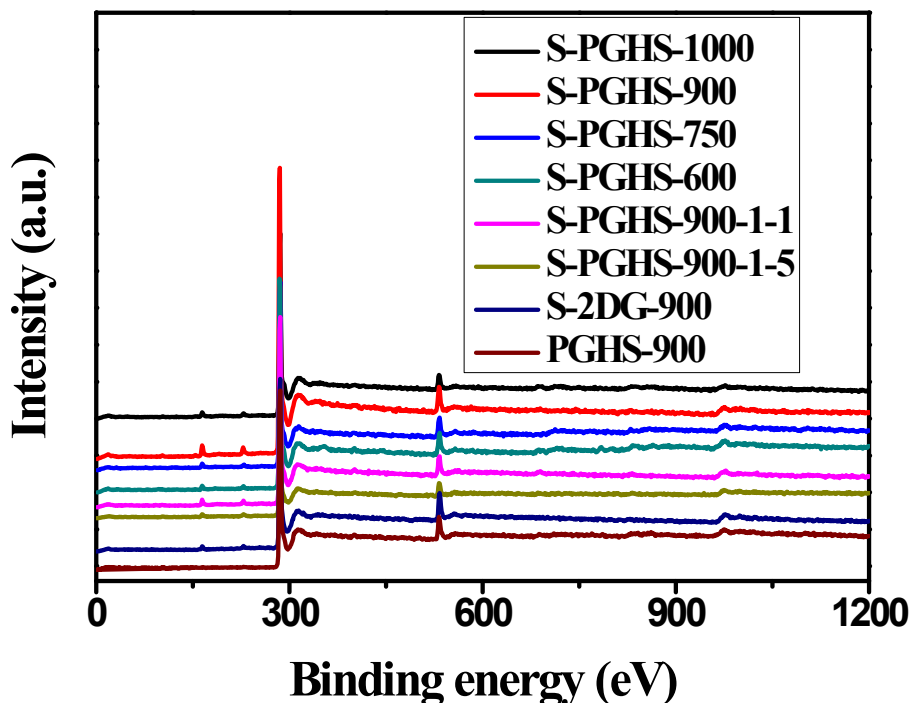


Fig. S4 XPS spectra of the different samples.

Table S2 The corresponding S content calculated from the XPS spectra of the different samples (Fig. S4).

| Samples | S-PGHS-1000 | S-PGHS-900 | S-PGHS-750 | S-PGHS-600 | S-PGHS-900-1-1 | S-PGHS-900-5-1 | S-2DG-900 | PGHS-900 |
|---------------|-------------|------------|------------|------------|----------------|----------------|-----------|----------|
| S content wt% | 1.19 | 1.99 | 1.01 | 0.78 | 1.23 | 1.14 | 1.1 | 0 |

Table S3 ICP analysis on the S-PGHS-900

| Elements | Fe | Mn |
|-------------------------|--------|---------|
| Content (mass fraction) | 0.043% | 0.0097% |

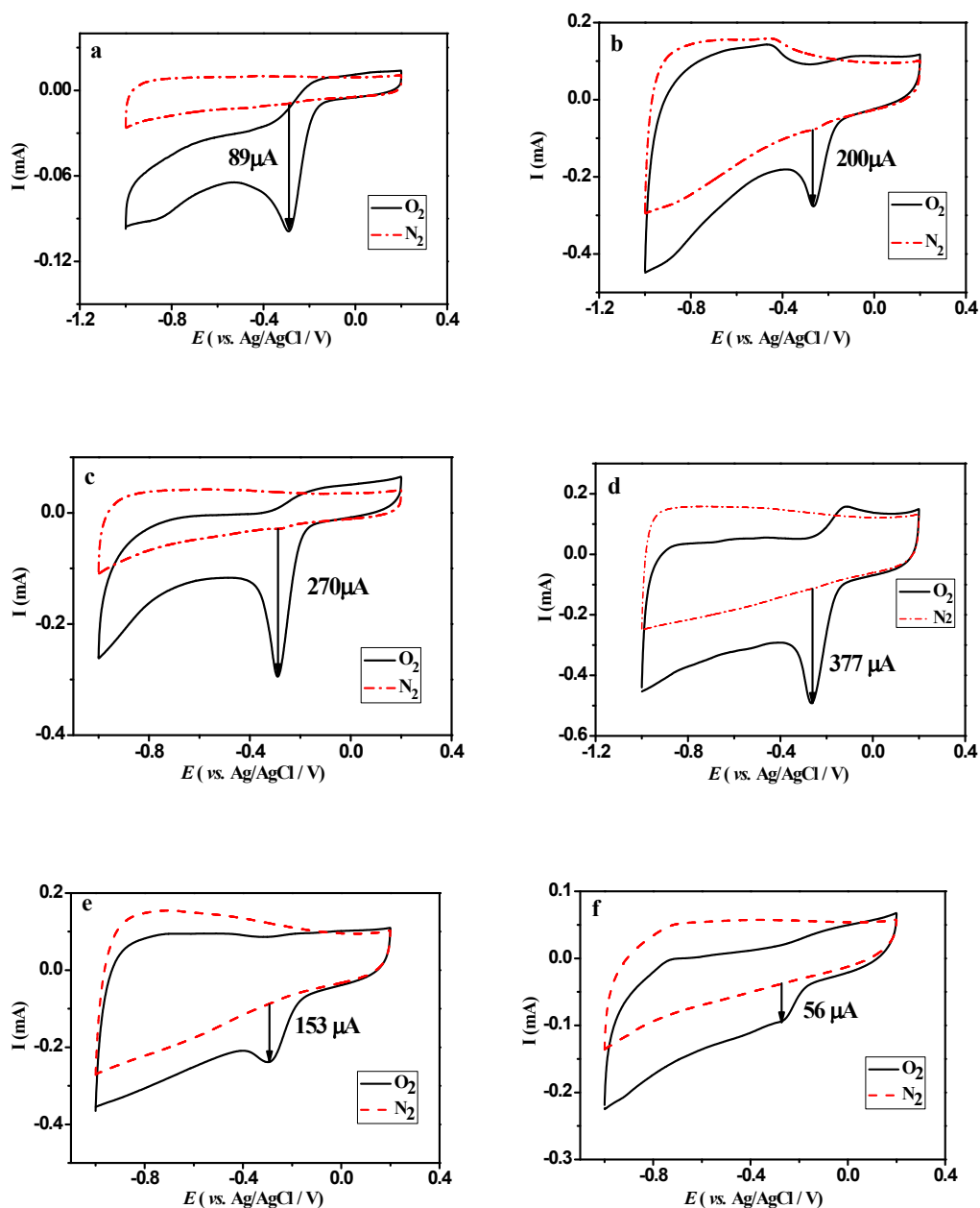


Fig. S5 CVs for the ORR of S-2DG-900 (a), S-PGHS-1-1-900 (b), S-PGHS-5-1-900 (c), S-PGHS-1000 (d), S-PGHS-750 (e) and S-PGHS-600 (f).

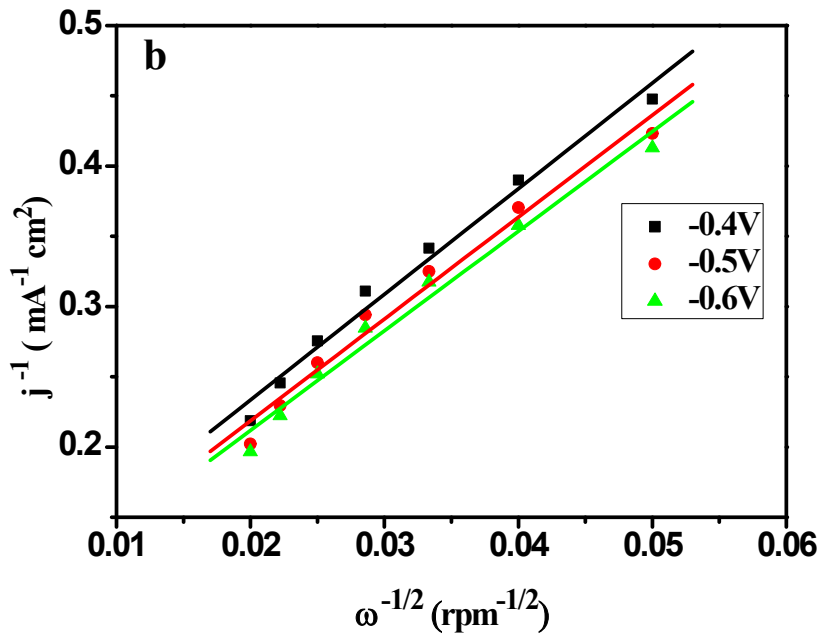


Fig. S6 Koutecky–Levich plot of J^{-1} vs $\omega^{-1/2}$ at different electrode potentials. The experimental data were obtained from (Fig. 6 a); the lines are linear regressions.

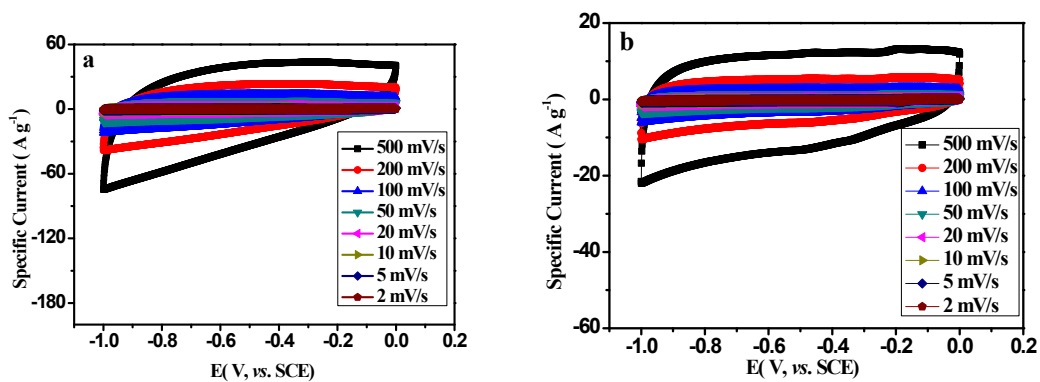


Fig. S7 CV curves of PGHS-900 (a) and S-2DG-900 (b) at different scan rates.

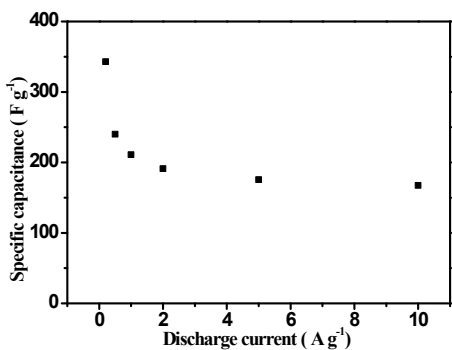


Fig. S8 Specific capacitance calculated from the corresponding discharge curves of S-PGHS-900 (Fig. 8e) for each current density.